Journal of Computing and Electronic Information Management
ISSN: 2413-1660 | Vol. 10, No. 1, 2023

State estimation and slug flow control of subsea production systems

Chuan Wang *, Xueliang Zhang, Huachuan Liu

Southwest Petroleum University, Chengdu, China

* **Corresponding author**: Chuan Wang

Abstract: The simulation and control of the severe slugging flow in the subsea multiphase pipeline is the focus of research in the production and exploitation of oil companies. Severe slug flow results in severe fluctuations of pressure and flow rate at both the wells end and the receiving host processing facilities, causing safety and shutdown risks. To prevent the severe slugging flow regime in multiphase transport pipelines, an ODE model is established by using the mass conservation law for individual phases in the pipeline and the riser sections. Then, the proposed model is compared to the results from the OLGA simulation. A comparative study of different slugging flow control solutions is conducted. Extended Kalman Filter (EKF), Back Propagation Neural Network (BPNN) and EKF&BPNN are used for state estimation and combined with PI controller. The EKF and BPNN are good nonlinear filters. However, when the nominal choke opening is increased, they work unsatisfying. The EKF&BPNN observer shows slightly better results than EKF and BPNN when the system has high input disturbance.

Keywords: ODE model; EKF; BPNN; Slug control.

1. Introduction

In the process of offshore oil and gas development, the mixed fluids produced from oil wells are usually transported to offshore platforms for processing. With the advancement of offshore oil and gas development technology, offshore oil and gas production is gradually carried out to deeper waters. For further development of offshore oil and gas, researchers have gradually focused their research and development on the technology of subsea oil and gas oil and gas separation. Many solutions have been proposed, such as the Marimba-provided VASPS, Perdido's BC-10 system and Rordis' SSBI system [1-5]. In all of these solutions, subsea separation technology is used, where oil, water and gas are separated and then transported over long distances using a mixture of oil and gas phases. In this way, the cost of offshore oil and gas development can be reduced.

Severe slugging in multiphase transportation is often a serious problem. For the control of severe slugging, researchers have proposed schemes based on top choke valve and gas lift. Due to the special characteristics of offshore oil and gas development, automatic control using the top-side choke valve is a recommended anti-slug solution. Instead of complex models, a simple dynamical model is required. Jahanshahi showed that the "Kaasa model" and "Di Meglio model" are able to demonstrate a good fit in expense of using more tuning parameters. However, finding parameter values is difficult. The "Nydal model" and " Eikrem model" are simple but cannot be matched with OLGA model. For this reason, an ODE model is established by extending the mass conservation model in the pipe [6].

Jahanshahi showed that the best observed solution for slugging control using a top choke valve is to use the bottom pressure and top flow rate of riser [7]. In the case of offshore production where the pipeline is placed in a harsh environment that does not allow direct measurements, one possible solution for slugging control is to use the top pressure and flow rate to estimate the pipeline condition and thus perform anti-slug control. If only top pressure measurements are available, the traditional control solution is to design an observer that uses the top pressure measurements to estimate the system state including the bottom pressure and then uses these estimates for control [8]. Extended Kalman filters have been used to estimate bottom pressures and other state variables in gas lift wells [9]. Using the Kalman filter for state estimation is not a bad solution.

Meglio proposed a nonlinear Luenberger-type observer that uses only the top pressure to reproduce the oscillations of the riser-slugging instability and then uses it for anti-slug control of a pipeline-riser system in experiments [10]. The observer was designed based on a simplified three-state model of the system. A follow-up study found that the peak of the sensitivity transfer function of the top pressure was not large and that Meglio did not impose restrictions on controllability [11]. The use of top pressure observation is only applicable for small valve openings and when using top pressure, we cannot open the valve at large production rates [12].

In recent years, neural networks have been widely used for system state estimation. A new method for subsea pipeline pressure state estimation by combining data-driven neural networks and traditional filters is proposed. Neural networks have good function approximation ability and have wide application in feature extraction and pattern recognition. With the development of technology, neural networks have been widely used in state estimation. A new state estimation method of the Bayesian filter-based EKF algorithm and BPNN to build a neural network model is proposed in this paper. It uses function as the excitation function combined with historical data to estimate the subsea pressure while integrating the state estimation of ODE model.

The simplified dynamical model proposed by Jahanshahi is extended in Section 2 and its practical feasibility is verified [6]. The ODE model is used for controller and observer design and the state estimation method of EKF&BPNN to obtain an estimate of the subsea pipeline pressure in section 3. The scheme proposed is validated and compared with the conventional control method in section 4. The results are

concluded in Section 5.

2. Pipeline Dynamical Model

2.1. Dynamical model

In the multiphase transport of the long-distance pipeline, severe slugging may also occur in the pipeline. In order to study the controllability and control characteristics of the system slugging, a simple physical model is established in Figure 1. The model includes a section of subsea horizontal pipeline, subsea down dip pipeline and riser section and a small section of platform horizontal pipeline.

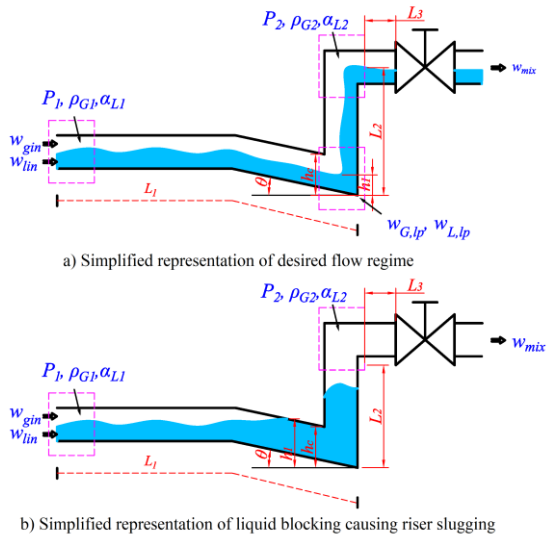


Figure 1. Pipeline-riser system with critical parameters

The ODE model used in this paper is based on the conservation of mass in all phases of the pipeline and riser, and its equation of state is:

$$\begin{aligned}\frac{dm_{G1}}{dt} &= w_{G,in} - w_{G,lp}\\ \frac{dm_{L1}}{dt} &= w_{L,in} - w_{L,lp}\\ \frac{dm_{G2}}{dt} &= w_{G,lp} - w_{G,out}\\ \frac{dm_{L2}}{dt} &= w_{L,lp} - w_{L,out}\end{aligned} \tag{1}$$

The four state variables in the model are:

m_{G1} : the mass of gas in the subsea pipeline

m_{L2} : the mass of liquid in the subsea pipeline

m_{G2} : the mass of gas in the riser

m_{L2} : the mass of liquid in the riser

Inflow conditions

The inlet boundary conditions usually change. The liquid volume fraction in pipeline section can be obtained based on the liquid mass fraction and densities of the two phase：

$$\alpha_{L,u} = \frac{\alpha_{Lm}/\rho_L}{\alpha_{Lm}/\rho_{L,h} + (1-\alpha_{Lm})/\rho_G} \tag{2}$$

The average liquid mass fraction in the pipeline section can be attained using the inflow boundary condition：

$$\bar{\alpha}_{Lm1} \cong \frac{w_{L,in}}{w_{G,in} + w_{L,in}} \tag{3}$$

Combing the two above equations gives the average liquid volume fraction in the pipeline：

$$\bar{\alpha}_{L1} \cong \frac{\bar{\rho}_{G1,\,p} w_{L,in}}{\bar{\rho}_{G1,p} w_{L,in} + \rho_L w_{G,in}} \tag{4}$$

In equation(4), the gas density can be calculated based on the nominal pressure (steady-state) of the pipeline:

$$\bar{\rho}_{G1,\,p} = \frac{P_{1,sta} M_G}{RT_1} \tag{5}$$

Outflow conditions

After the long transport pipeline reaches the offshore platform, its external boundary pressure is constant (separator pressure). The constant pressure condition and the choke valve model are used as the boundary conditions at the outlet of the riser.

$$w_{mix} = f(z)\sqrt{\rho_t (P_2 - P_0)} \tag{6}$$

Were z ∈ (0, 1) and f(z) is the equation for the opening of the valve. A linear valve and is assumed in the simulation model (i.e. f(z) = z).

The equation of gas and liquid outflow is.

$$w_{L,\text{out}} = \alpha_{Lm,t} w_{\text{mix}} \tag{7}$$

$$w_{G,\text{out}} = (1 - \alpha_{Lm,t}) w_{\text{mix}} \tag{8}$$

In order to calculate the mass flow rate of each phase in the outlet model in equations (7)and (8), also the mixing density ρ_t, used in equation (6), the phase distribution at the top of the riser must be known.

Liquid mass fraction at the outlet choke valve:

$$\alpha_{Lm,t} = \frac{\alpha_{L,t}\rho_{L,\,p}}{\alpha_{L,t}\rho_{L,p} + (1-\alpha_{L,t})\rho_{G2}} \tag{9}$$

Density of the two-phase mixture at the top of the riser:

$$\rho_{t,\,r} = \alpha_{L,t}\rho_{L,r} + (1-\alpha_{L,t})\rho_{G2} \tag{10}$$

The above equation αL,t is the liquid volume fraction at the top of the riser. The pressure and liquid volume fraction between the vertical gravity-dominated two-phase flow pipes are approximately linear for the desired steady flow state. The pressure gradient along the riser can be assumed to be constant. Due to the assumed linear relationship, the liquid volume fraction also maintains an approximately constant gradient along the riser for a steady flow state.

$$\frac{\partial \alpha_{L2}}{\partial y} = constant \tag{11}$$

This assumption indicates that the volume fraction of the liquid in the middle of the riser is the average of the volume fractions at both ends of riser. On the other hand, the volume fraction of liquid in the middle of the riser is approximately equal to the average volume fraction of liquid in the riser given by (28). Therefore,

$$\bar{\alpha}_{L2} = \frac{\alpha_{L,lp} + \alpha_{L,t}}{2} \tag{12}$$

The liquid volume fraction αL,lp at the bottom of the riser is determined by the flow area of the liquid phase at the low point.

$$\alpha_{L,lp} = \frac{A_L}{\pi r_1^2} \tag{13}$$

Therefore, the liquid volume fraction αL,t at the top of the riser can be expressed as:

$$\alpha_{L,t} = 2\bar{\alpha}_{L2} - \alpha_{L,lp} = \frac{2m_{L2}}{V_2\rho_{L,\ r}} - \frac{A_L}{\pi r_1^2} \tag{14}$$

c)Pipeline model

In the pipeline, the gas and liquid are often unevenly distributed. In this case, the mass of the liquid in the pipeline is given by $\bar{m}_{L1} = \rho_L V_1 \bar{\alpha}_{L1}$. The lowest point of the pipeline level at the bottom of the riser can be defined as $\bar{h}_1 \cong h_c \bar{\alpha}_{L1}$. If the mass of the liquid in the pipeline increases, the level at the bottom of the riser will also change, and its position changes have the following relationship.

$$\begin{aligned} &\Delta h_1 = \Delta L \sin(\theta) \\ &\Delta m_{L1} = \Delta L \pi r_1^2 (1-\bar{\alpha}_{L1})\rho_L \\ &h_1 = \bar{h}_1 + \Delta L \sin(\theta) \\ &h_1 = \bar{h}_1 + \frac{\Delta m_{L1}}{\pi r_1^2 (1-\bar{\alpha}_{L1})\rho_L}\sin(\theta) \\ &\bar{h}_1 = K_h h_c \bar{\alpha}_{L1} \end{aligned} \tag{15}$$

Where Kh is the correction factor around unity which can be used for fine-tuning of the model.

Therefore, the liquid level of h1 in the pipeline can be expressed as a function of the liquid mass mL1 in the pipe. The functional relationship can be expressed as:

$$h_1 = K_h \bar{h}_1 + \left(\frac{m_{L1} - \rho_{L,r} V_1 \bar{\alpha}_{L1}}{\pi r_1^2 (1-\bar{\alpha}_{L1})\rho_L}\right)\sin(\theta) \tag{16}$$

Where mL1 is the state variable of the model. The remaining parameters are constant.

Volume occupied by the gas in the pipe:

$$V_{G1} = V_1 - (1-\alpha_{L,t}) m_{L1}/\rho_{L,\ r} \tag{17}$$

Gas density in pipeline:

$$\rho_{G1} = \frac{m_{G1}}{V_{G1}} \tag{18}$$

Pressure in pipeline assuming ideal gas：

$$P_1 = \frac{\rho_{G1} R T_1}{M_G} \tag{19}$$

For the pressure loss due to friction in the pipeline, only the friction of the liquid is considered.

$$\Delta P_{fp} = \frac{\bar{\alpha}_{L1}\lambda_p \rho_L \bar{U}_{sl,in}^2 L_1}{4r_1} \tag{20}$$

The correlation for turbulence flow in smooth wall pipes is used as the friction factor in the pipeline.

$$\lambda_p = 0.0056 + 0.5\mathrm{Re}_p^{-0.32} \tag{21}$$

Reynolds number in pipeline:

$$\mathrm{Re}_p = \frac{2\rho_L \bar{U}_{sl,in} r_1}{\mu} \tag{22}$$

Where μ is the liquid viscosity and Usl,in is the surface velocity of the inlet liquid:

$$\bar{U}_{sl,in} = \frac{w_{L,in}}{\pi r_1^2 \rho_L} \tag{23}$$

d)Riser model

Total volume of riser:

$$V_2 = \pi r_2^2 (L_2 + L_3) \tag{24}$$

Volume occupied by gas in riser:

$$V_{G2} = V_2 - m_{L2}/\rho_L \tag{25}$$

Density of gas at top of the riser:

$$\rho_{G2} = \frac{m_{G2}}{V_{G2}} \tag{26}$$

Pressure at top of the riser:

$$P_2 = \frac{\rho_{G2} R T_2}{M_G} \tag{27}$$

Average liquid volume fraction in riser:

$$\bar{\alpha}_{L2} = \frac{m_{L2}}{V_2 \rho_L} \tag{28}$$

Average density of mixture inside riser:

$$\bar{\rho}_m = \frac{m_{G2} + m_{L2}}{V_2} \tag{29}$$

Friction loss in riser

$$\Delta P_{fr} = \frac{\bar{\alpha}_{L2}\lambda_r \bar{\rho}_m \bar{U}_m^2 (L_2 + L_3)}{4r_2} \tag{30}$$

Friction factor of riser using same correlation as pipeline:

$$\lambda_r = 0.0056 + 0.5\mathrm{Re}_r^{-0.32} \tag{31}$$

Reynolds number of flow in riser:

$$\mathrm{Re}_r = \frac{2\bar{\rho}_m \bar{U}_m r_2}{\mu} \tag{32}$$

Riser fluid mixing speed:

$$\bar{U}_m = \bar{U}_{sl2} + \bar{U}_{sg2} \tag{33}$$

Among them:

$$\begin{aligned} \bar{U}_{sl2} &= \frac{w_{L,in}}{\rho_L \pi r_2^2} \\ \bar{U}_{sg2} &= \frac{w_{G,in}}{\rho_{G2} \pi r_2^2} \end{aligned} \tag{34}$$

e) Gas flow model at the bottom of the riser.

When the liquid height in the bottom of the riser exceeds the critical level（h1>hc), slugging will occur at the bottom of the riser and the gas flow rate is zero.

$$w_{G,lp} = 0, \quad h_1 \geq h_c \tag{35}$$

When the liquid is not blocked at the bottom of the riser（h1<hc), the gas will flow from volume VG1 to VG2 with a mass flow rate of wG, lp. According to the physical model, the two most important parameters that determine the gas rate are the pressure drop over the low-point and the opening area. This suggests that the flow of gas can be approximated by a valve flow model. The pressure drop drives the gas through an opening area of AG.

$$w_{G,lp} = K_G A_G \sqrt{\rho_{G1}\Delta P_G}, \quad h_1 < h_c \tag{36}$$

Among them:

$$\Delta P_G = P_1 - \Delta P_{fp} - P_2 - \bar{\rho}_m g L_2 - \Delta P_{fr} \tag{37}$$

f) Liquid flow model at the bottom of the riser.

The liquid at the bottom of the riser can also be used in a similar way to the equation for the gas at the bottom of the riser.

$$w_{L,lp} = K_L A_L \sqrt{\rho_L \Delta P_L} \tag{38}$$

Among them:

$$\Delta P_L = P_1 - \Delta P_{fp} + \rho_L g h_1 - P_2 - \bar{\rho}_m g L_2 - \Delta P_{fr} \tag{39}$$

The area of the gas flow is calculated exactly using some trigonometric functions. For simplicity, a quadratic approximation is used in the proposed model.

$$A_G \cong \pi r_1^2 \left(\frac{h_c - h_1}{h_c}\right)^2, \quad h_1 < h_c \tag{40}$$

$$A_L = \pi r_1^2 - A_G \tag{41}$$

2.2. Model validation

The model developed in this paper is solved using ode15s provided by matlab as a solver. The OLGA model is also established using the same conditions in Figure. 2. The total length of the pipeline is 5000 m, diameter 0.12 m, including 2000 m horizontal pipeline and 3000 m downward inclined pipeline, The length of the riser is 300 m, diameter 0.1 m, and the upper part of the riser has 100 m horizontal pipeline.

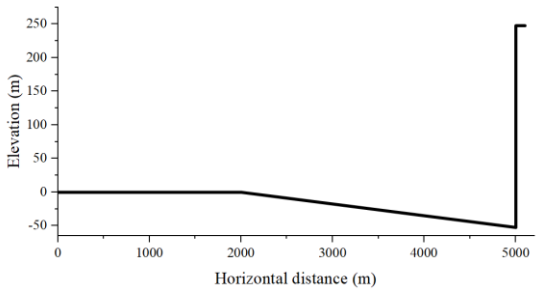


Figure 2. OLGA model

The ODE model is compared with the OLGA model at different valve openings. When the valve opening exceeds the critical value, the horizontal pipe pressure P1, the top pressure of the riser P2 and the outlet flow rate W will be oscillating, as shown in Figure3. The upper line represents the maximum value in the oscillation process and the lower line represents the minimum value.

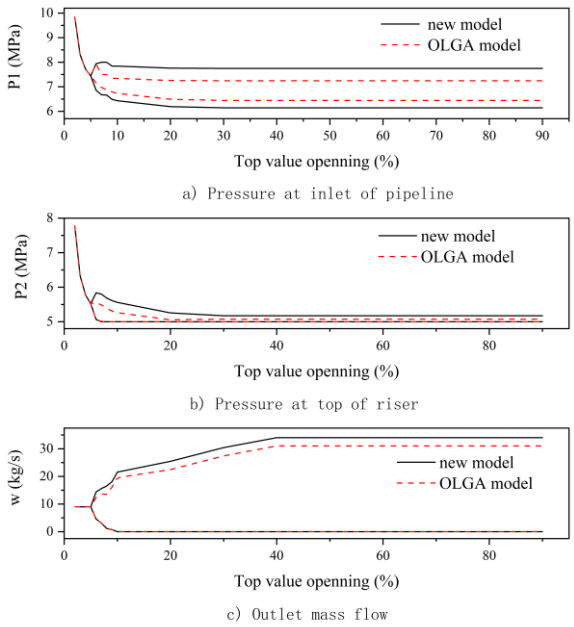


Figure 3. Model comparison bifurcation diagram

As can be seen from the Figure 3, the instability threshold of both models is 5%. The maximum and minimum values of the oscillation are also close to each other. Compared with the OLGA model, the ODE model is simpler and its calculation speed is faster, which is more suitable for slugging control.

3. State Estimation Method Based On EKF&BPNN

3.1. Control system

3.1.1. Controller structure

In this work, we use the ODE model presented in Section 1.1 for observer and control design. As shown in Figure 4, an observer is needed to estimate the state variables of the system and use the estimates for state feedback. The separation principle allows us to split the design into two tasks. First, a state feedback controller is designed to stabilize the system and meet other design specifications. Then, the output feedback controller is obtained by replacing the state x by its estimate $\hat{x}$ provided by the observer.

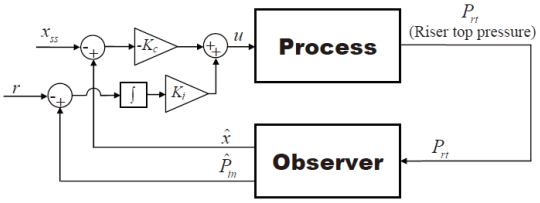


Figure 4. Feedback control block diagram

3.1.2. Feedback control structure

As shown in Figure 4, the complete state feedback is applied by using the estimated state. In addition, to prevent deviation from the operating point, the integral action is added by integrating the set point deviation from the estimated subsea pressure (P_{in}). The total control action can be expressed as:

$$u(t) = -K_c(\hat{x}(t) - x_{ss}) + K_i\int_0^t \left(\hat{P}_{in}(\tau) - r\right)d\tau \quad (42)$$

Here, Kc is the linear optimal controller calculated by solving the Riccati equation, and K_i is the relatively small integral gain.

3.2. Extended Kalman Filter

The underwater production system can be described using a state space model. The state x in the system is represented by a finite dimensional vector. The state space usually consists of two models, a process model and a metric model. The first model is a dynamic representation that describes how the state propagates in time as a function of external inputs, also known as the state model, and the second model describes how the numerical measurement vector y is related to the process state, also known as the measurement model. The state-space equations of a system in nature are generally continuous and nonlinear. However, such models are often difficult to solve. Therefore, in practical engineering, the system state space equations are generally formulated as discrete nonlinearities, as shown in the following equation.

$$x_k = f(x_{k-1}, u_{k-1}) + v_{k-1} \quad (43)$$

$$y_k = h(x_k, u_k) + w_k \quad (44)$$

Where vk-1 is a vector of Gaussian zero-mean process noise, representing model error and disturbance. wk is a vector of Gaussian zero-mean measurement noise. The state vector is assumed a random variable with mean value xk-1 and covariance matrix pk-1. After a nonlinear transformation of f, the random variable xk is obtained using the recursive data to further estimate the system state and thus the subsea pipeline pressure.

In this paper, we use EKF as an observation scheme to observe the system state. EKF is a Taylor expansion of a nonlinear model of a nonlinear system, and the expanded equations are truncated at a specified order, usually the truncation order of the system is one order. Using this truncation method can greatly reduce the computational effort of the system. When the nonlinear system is represented as a

linear system, the system can be described as

$$x_k = Ax_{k-1} + Bu_k + w_k$$
$$y = Hx_k + v_k \tag{45}$$

The EKF does not require large number of samples and has predictive and corrective properties. The computational process does not discretize the model or the observer system, using Matlab (ode15s solver) to integrate the model to solve the state vector from time *k-1* to *k*. The EKF algorithm is formulated as:

$$\hat{X}_{k-1} = [\hat{x}_{k-1} \ \ldots \ \hat{x}_{k-1}] + \sqrt{c}\left[\sqrt{P_{k-1}} \ -\sqrt{P_{k-1}}\right]$$
$$\hat{X}_k = f\left(\hat{X}_{k-1}, u_{k-1}\right)$$
$$\hat{x}_k^- = \hat{X}_k W_m$$
$$P_k^- = \hat{X}_k W_c \left[\hat{X}_k\right]^T + Q_{k-1}$$
$$\hat{X}_k^- = [\hat{x}_k^- \ldots \hat{x}_k^-] + \sqrt{c}\left[\sqrt{P_k^-} \quad -\sqrt{P_k^-}\right]$$
$$Y_k^- = h\left(\hat{X}_k^-\right)$$
$$\mu_k = Y_k^- W_m$$
$$S_k = Y_k^- W_m [Y_k^-]_T^T + R_k$$
$$C_k = \hat{X}_k^- W_c [Y_k^-]^T$$
$$K_k = C_k S_k^{-1}$$
$$\hat{x}_k = \hat{x}_k^- + K_k [y_k - \mu_k]$$
$$P_k = P_k^- - K_k S_k K_k^T$$
$$P_1 = h_{(P_1)}(\hat{x}_k, u_k)$$

3.3. Back Propagation Neural Network design

3.3.1. Data normalization

In this study, the values and units of the pressure, flow rate, and valve opening have a large gap, which requires normalization of the data. The normalization method using linear mapping is used with the following algorithm.

$$x' = \begin{cases} 0, & x < x_{\min} \\ \dfrac{x - x_{\min}}{x_{\max} - x_{\min}}, & x_{\min} \le x \le x_{\max} \\ 1, & x > x_{\max} \end{cases} \tag{46}$$

Where x' is the normalized processed data and x is the original measurement. xmin and xmax are the minimum and maximum values of the original data respectively. In the experiment, the historical data produced in the training are the valve opening u, the pressure at the bottom of the subsea pipeline P1, the pressure at the top of the riser P2, and the outlet flow rate wout.

3.3.2. Back Propagation Neural Network

Currently, BPNN is actively researched, and their main structures are: loose structure and delicate structure. It does not change the neural network structure using elements instead of neurons. Compared with traditional neural networks, it is more flexible and effective and has good realization in dealing with nonlinear problems. In this paper, the pressure of the subsea pipeline will be estimated by the good fitting ability of the BPNN, so that the feedback system has better state estimation ability. The structure is shown in Figure 5.

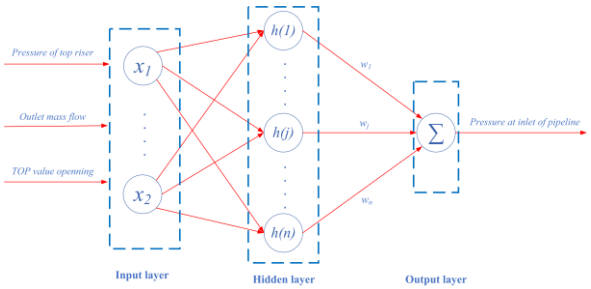


Figure 5. BPNN structure

1) Input layer: the data collected by the sensors (undersea sensor data when available) P2, wout, u are normalized and used as inputs for training.

2) Hidden layer: the Morlet wavelet function is used as mother wavelet function. The Morlet wavelet function is continuous derivable with good time-frequency local characteristics and relatively simple expression. Its mathematical formula is:

$$y = \cos(1.75x)\mathrm{e}^{-x^2/2} \tag{47}$$

By adding the translation and scaling factors, the output of each node can be expressed as:

$$h(j) = h_j\left(\frac{\sum_{i=1}^{k} \omega_{ij} x_i - b_j}{a_j}\right) \quad j = 1, 2, \cdots, l \tag{48}$$

where hj is the jth neuron activation function and bj is the translation factor, and aj is the scaling factor.

3) Output layer: The BPNN output layer can be expressed as:

$$y(k) = \sum_{i=1}^{l} \omega_{ik} h(i) \quad k = 1, 2, \cdots, m \tag{49}$$

4) parameter update: the BPNN uses weight correction algorithm similar to BPNN, using gradient to correct the its weights and the parameters, so that the BPNN continuously approximates the desired output. The MSE is used as the error function, and its iterative process can be expressed as follows.

Calculation error:

$$MSE = \frac{1}{M}\sum_{m=1}^{M}(y_m - \hat{y}_m)^2 \tag{50}$$

Correction parameters:

$$\omega_{n,k}^{(i+1)} = \omega_{n,k}^{i} + \Delta\omega_{n,k}^{(i+1)}$$
$$a_k^{(i+1)} = a_k^{i} + \Delta a_k^{(i+1)} \tag{51}$$
$$b_k^{(i+1)} = b_k^{i} + \Delta b_k^{(i+1)}$$

$\Delta\omega_{n,k}^{(i+1)}, \Delta a_k^{(i+1)}, \Delta b_k^{(i+1)}$ calculated from the error can be expressed as:

$$\Delta\omega_{n,k}^{(i+1)} \quad -\eta\frac{\partial e}{\partial \omega_{n,k}^{(i)}}$$
$$\Delta a_k^{(i+1)} \quad -\eta\frac{\partial e}{\partial \alpha_k^{(i)}} \tag{52}$$
$$\Delta b_k^{(i+1)} \quad -\eta\frac{\partial e}{\partial b_k^{(i)}}$$

where η is the learning rate. For the actual training of the network, when the subsea sensor is available, the data is used including P1, P2, w and the top valve opening u. The neural network is trained using P1(k-1), P2(k)， w(k) and u(k) as input and P1(k) as output.

4. Method Effectiveness and Evaluation.

In order to verify the stability of the control system, we used the model established above, and tried to verify the open-loop system. Here, only EKF was used as the observation scheme. Based on the model established in the previous section, the bottom pressure of the two Wells remained stable, and the valve operating point was set at 12%. Set the variance between the top pressure and flow noise as the observed mean of 0.33%. The collected measurement values are used inside the control system to estimate the pressure of the submarine pipeline and then control it. Although we did not directly use the direct measurement value of P1 in the experiment, we still added a white noise with an average value of 0 and variance as the measurement value of 0.33% to replace the measurement value of the sensor for comparison with the estimated effect. The controller is a simple PI controller as the controller.

As can be seen from the results of Figure 6, when only EKF was used as an observation scheme for control, the system showed a tendency of oscillation within a certain range. Simple control method and can effectively achieve the effect of stable control.

The system uses a PI controller as the control scheme. The controller is turned on at the initial moment to estimate the state of the system using two different observation schemes. The results are shown in Figure 7, Figure 8 and Figure 9, where the black line represents the different observation schemes and the red line represents the actual value of the system at this time. The MSE between the system settings and the actual values for the different observation schemes is also calculated. The results are shown in Table 1.

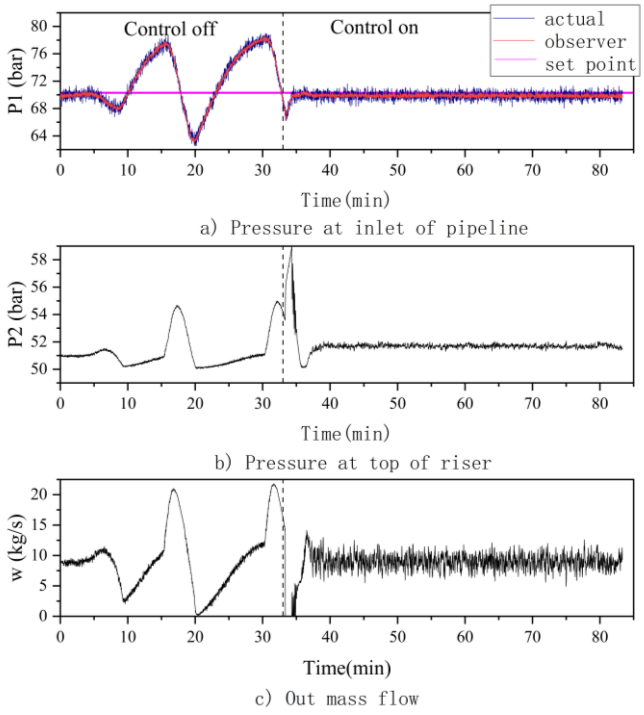


Figure 6. Open-loop system control characteristics

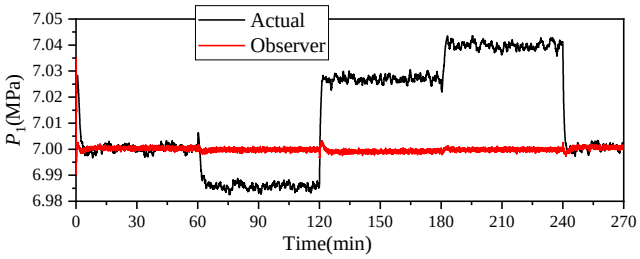


Figure 7. EKF as observer

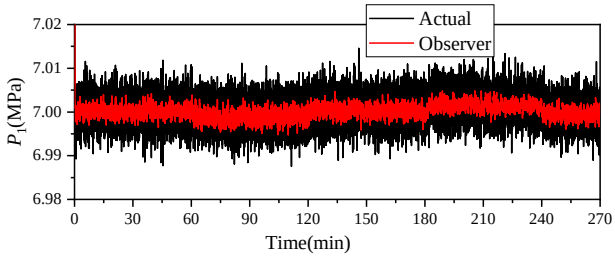


Figure 8. BPNN as observer

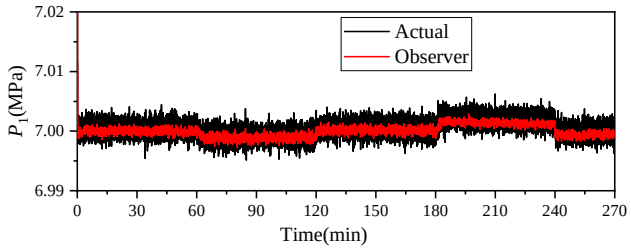


Figure 9. EKF&BPNN as observer

Table 1. MSE of different observation methods

Estimation Method	MSE
EKF	0.67
BPNN	0.53
EKF&BPNN	0.12

It can be seen that both observation methods can achieve stable control of the inlet pressure within a certain range. But better control can be obtained using the observation scheme of EKF&BPNN. The figure reflects that the BPNN&EKF observation scheme will provide a more accurate estimate of the system in the presence of disturbances in the system input. For a period of smooth inputs, there is no doubt that the EKF can easily provide accurate estimates. But its ability to follow the system is weaker when the input changes. In contrast, the observer method of BPNN&EKF provides more accurate state estimates. The MSE between the actual value and the set value is smaller.

5. Conclusions

In this paper, through the research and analysis of the severe slugging flow in the long-distance pipeline of the subsea production system, the ODE model was established by using the law of conservation of mass in the two-phase in the pipeline. Compared with the OLGA model, it was found that the valve critical values of both are consistent and the maximum and minimum values of the oscillation are close. The reasonable simplification of the ODE model greatly reduces the calculation time. It is more suitable for the subsequent design of the controller and observer.

Based on the model proposed, an observation system integrating EKF and BPNN is used to estimate the state of the

subsea oil and gas production system. Compared with EKF and BPNN, the observation system can better fit the relationship between top pressure, flow rate and valve opening with bottom pressure. The state estimation by incorporating the ODE model can improve the system state estimation results and provide more accurate estimation results for the controller to achieve the control of subsea slugging. The incorporation of neural networks can effectively improve the reliability of the control system, which is a guideline for oil and gas development under complex conditions.

References

[1] R Stromquist, Gustafson S. SUBSIS -- world's first subsea separation and injection system[J]. ABB Review, 1998, (No.6): 4-13.

[2] Massimo Benetti, Villa Marco. Two-phase separation/pumping to make subsea debut on Marimba. [J]. Offshore, 1998, (No.12): 46.

[3] J-H Neuenkirchen. Tordis Subsea Separation Boosting and Injection (SSBI) Project: Project Presentation and Description of the Production Control System[A]//Neptune, France: 2006.

[4] Chris Carpenter. Subsea Production Optimization in Field BC-10 Offshore Brazil. [J]. Journal of Petroleum Technology, 2016, (No.5): 67-69.

[5] M-L Euphemio, Lima I-F, Orlowski R, et al. Marlim SSAO 3-Phase Subsea Separation System: Project Overview and Execution Strategy[A]//Houston, TX(US): 2012.

[6] Esmaeil Jahanshahi, Skogestad Sigurd. Simplified Dynamical Models for Control of Severe Slugging in Multiphase Risers[J]. IFAC Proceedings Volumes, 2011, 44(1): 1634-1639.

[7] Esmaeil Jahanshahi, Skogestad Sigurd, Helgesen Anette-H. Controllability analysis of severe slugging in well-pipeline-riser systems[J]. IFAC Proceedings Volumes, 2012, 45(8): 101-108.

[8] Gisle-Otto Eikrem, Imsland Lars, Foss Bjarne. Stabilization of Gas Lifted Wells Based on State Estimation[J]. IFAC Proceedings Volumes, 2004, (No.1): 323-328.

[9] Gisle-Otto Eikrem, Aamo Ole-Morten, Siahaan Hardy, et al. Anti-Slug control of gas-lift wells - Experimental results[J]. IFAC Proceedings Volumes, 2004, (No.13): 799-804.

[10] F Di Meglio, Kaasa G-O, Petit N, et al. Reproducing slugging oscillations of a real oil well[A]//Atlanta, GA: 2010.

[11] F-A Di Meglio, Petit N-A, Alstad V-B, et al. Stabilization of slugging in oil production facilities with or without upstream pressure sensors (Article)[J]. Journal of Process Control, 2012, (No.4): 809-822.

[12] Florent Di Meglio. Production de pétrole: étude dynamique et contrôle des écoulements à bouchons[D]. Dynamical Systems [math.DS]. École Nationale Supérieure des Mines de Paris, 2011.